

Letter

Fourier analysis of high-spatial-frequency holographic phase gratings

I. BÁNYÁSZ*

Department of Crystal Physics, Research Institute of Solid State Physics
and Optics of the Hungarian Academy of Sciences, PO Box 49,
H-1525, Budapest, Hungary

(Received 23 September 2004; in final form 13 May 2005)

Plane-wave holograms were recorded on Agfa–Gevaert 8E75HD holographic plates, in a wide range of bias exposures and fringe visibilities. Plates were processed by developer AAC and bleaching agent R-9. Phase gratings were studied by phase-contrast microscopy, using a high-power immersion (100×) objective. Phase-contrast photomicrographs were Fourier analysed. Thus first-, second- and third-order modulations of the refractive index as functions of bias exposure and visibility of the recording interference pattern could be determined. Relative amplitudes of the higher-order modulations to that of the first-order modulation can serve as a measure of the nonlinearity of the holographic recording. The results presented here can be used to check the validity of grating profile calculations based on higher-order coupled-wave theory.

1. Introduction

The aim of this work was to obtain direct information on the nonlinearity of holographic recording material and processing via Fourier analysis of the holographic grating.

Holography is a relatively new way of imaging, since its principles were first published by its inventor Dénes Gábor [1] in 1948. It reconstructs the image of an object from a (photographically recorded) interferogram of the object wave and a coherent reference wave. An ideal hologram would reconstruct a perfect replica of the object wave. The principal limitation of holographic imaging is imposed by the laws of physical optics; the resolution of the reconstructed image is determined by the wavelength of the light and the numerical aperture (NA) of the hologram.

Besides other imperfections of holographic recording and reconstruction, such as aberrations due to misalignment of the reconstructing wave [2], the second most important, and very often neglected, factor that limits the quality of holographic

*Email: banyasz@sunserv.kfki.hu

imaging is the recording material itself. After a series of important and valuable studies on holographic materials published in the early years of laser holography, it was Lin [3] who proposed and developed a really useful concept and method for characterization of holographic materials. He used the so-called Lin curves for the characterization of holographic recording materials; the square root of the diffraction efficiency of plane-wave gratings, recorded in the material as a function of the bias exposure and fringe visibility at recording: $\sigma(E_0, V)$. An ideal recording material would respond linearly to the holographic exposure, so that Lin curves of an ideal holographic material are sets of lines. However, as Lin pointed out and demonstrated in his article, all real holographic materials are nonlinear, and their Lin curves can be considered to be quasilinear only locally. The concept of Lin curves applies for both amplitude and phase holograms.

The author of this article developed a method for the evaluation of the effects of material nonlinearity via incorporation of the Lin curves of holographic materials in the double Fresnel–Kirchhoff integral describing the full process of hologram recording and reconstruction [4]. He measured and published complete sets of Lin curves of silver halide materials, even completing the basic Lin function with a third independent variable: the spatial frequency of the plane-wave holographic grating [5]. So the complete Lin function describing nonlinearities of a holographic material is of the following form: $\sigma(E_0, V, \nu)$, where E_0 and V are the bias exposure and fringe visibility at recording respectively and ν is the spatial frequency of the grating.

In the above-mentioned methods, hologram recording and reconstruction were treated in the framework of transparency theory; that is, holograms were regarded as very thin phase, amplitude or mixed transparencies, and reconstruction was the result of diffraction of the reconstruction waves on those thin transparencies. It was Kogelnik [6] who proved that diffraction from volume gratings could not be described by transparency theory. The diffraction efficiency of such gratings has to be calculated using coupled-wave theory that describes correctly the interaction of the various diffraction orders *inside* the grating (hologram). First-order coupled-wave theory assumes a linear recording material, that is a sinusoidal grating profile, and the expression derived for the square root of the diffraction efficiency of a transmission phase hologram is

$$\sigma(\nu) = \left| \sin \left(\frac{\pi \Delta n d}{\lambda \cos[\arcsin(\nu\lambda/2)]} \right) \right|, \quad (1)$$

where ν is the spatial frequency of the grating, Δn is the modulation of the refractive index, d is the hologram thickness and λ is the wavelength of the light. So, if one knows $\Delta n(E_0, V, \nu)$, σ can be calculated using equation (1). However, as we emphasized above, real holographic materials *do not* respond linearly to the holographic exposure, and that means in the coupled-wave theoretical treatment of holography that holographic gratings do not have a pure sinusoidal profile. The effects of higher-order harmonics in volume holographic gratings have been studied by various workers [7–9]. It was Solymar and his co-workers [9] who developed a numerical method for computing diffraction efficiencies of volume holograms that have higher-order harmonics in their refractive index profile. Based on their

precise experiments of diffraction efficiency measurements, they deduced that even fourth-order harmonics should exist in strongly modulated gratings. The aim of the present work was to measure directly the $\Delta n_1(E_0, V)$, $\Delta n_2(E_0, V)$ and $\Delta n_3(E_0, V)$ characteristics of the material, that is the dependences of the first-, second- and third-order harmonics of the refractive index modulation of the holographic gratings on the bias exposure and the visibility of the recording interference pattern for a fixed spatial frequency and processing, using phase contrast microscopy and Fourier analysis.

Phase-contrast microscopy, invented by Zernicke [10], was used in these experiments. This powerful method for the observation of transparent microobjects was improved by others. Contributions made by Françon [11–13] were especially important.

Kostuk and Goodman [14] used phase-contrast microscopy to prove the existence of a spatial-frequency-dependent diffusion process in the fixation-free rehalogenating bleach of holograms recorded in Agfa 8E75HD emulsion at low (up to 100 line pairs per millimetre (lp mm^{-1})) spatial frequencies.

It was the author of this article who first tried to apply phase-contrast and interference microscope to a *quantitative* study of phase gratings. Systematic study of phase gratings fabricated via ion implantation in glass both with interference- and phase-contrast microscopies was performed by the author of the present article and his co-workers [15]. In those experiments the highest spatial frequency of the implanted gratings was 250 lp mm^{-1} .

Semiphysically developed phase holograms in Agfa 8E75HD emulsion were also studied by the present author using phase-contrast microscopy [16]. It was proved that phase-contrast microscopy could be used for the quantitative determination of refractive index modulation in holographic phase gratings [17].

2. Hologram recording

Detailed description of the recording conditions and the diffraction efficiency measurements were published earlier [18]. They are summarized briefly here. Plane-wave holograms were recorded in Agfa–Gevaert 8E75HD plates with a helium–neon laser operating at 632.8 nm. The spatial frequency of the gratings was $\nu = 1200 \text{ lp mm}^{-1}$. Holograms at seven values of fringe visibility, namely at $V = 0.2, 0.4, 0.6, 0.8, 0.9, 0.95$ and 1.0 were recorded. Twelve holograms at exposures ranging from $10 \mu\text{J cm}^{-2}$ to 1.3 mJ cm^{-2} were recorded at each visibility. Holograms have been developed with AAC developer and bleached in R-9 solvent bleach.

Use of the Agfa–Gevaert 8E75HD recording material, which is no longer being produced, in these experiments can be justified by the fact that currently available silver halide emulsions of similar parameters, that is silver halide grain size distribution, sensitisation and emulsion quality, must have similar $\Delta n_1(E_0, V)$, $\Delta n_2(E_0, V)$ and $\Delta n_3(E_0, V)$ characteristics, too. Specifications of PFG-02 holographic plates, fabricated by Slawich (Russia), and of FT340T/SP696T plates, fabricated by Ilford, are very close to those of Agfa–Gevaert 8E75HD. Very thorough and detailed

treatment of these commercial holographic materials can be found in chapter 3 of the monograph by Bjelkhagen [19].

3. Microscopic study of the holograms

The microscope used in the measurements was a Nikon Labophot 2 with a phase-contrast attachment. Each hologram was observed using a phase-contrast microscope objective. The objective was a CF N Plan DL 100X immersion type one with an NA of 1.25 and a focal length of 1.71 mm. The refractive index of the cedar wood oil was $n_{\text{oil}} = 1.515$ at the D line of sodium at 23°C. A green interference filter centred at $\lambda = 540$ nm was used. The measurements yielded only the optical path variations due to the index-of-refraction grating (assuming a good match of the index of refraction between the emulsion and the oil).

Each phase-contrast micrograph was recorded photographically, using the Microflex photomicrographic attachment of the Labophot 2 microscope and Kodak HR12 (ISO 100) films. It was possible to set automatically the exposure times to maintain bias exposure at the middle of the quasilinear range of the D -log E curve of the photographic emulsion. The photomicrographs were scanned in a special high-resolution scanner and stored in files.

According to the theory of phase-contrast microscopy, the phase difference in a phase-contrast micrograph is

$$\phi = \frac{\gamma}{2}, \quad (2)$$

where ϕ is the phase difference in radians and γ is the measured contrast of the phase object [13]. However, especially when fine objects (gratings of high spatial frequency in this case) are studied, one has to take into account the modulation transfer function (MTF) of the microscope objective, too. According to the theory developed by Françon [12, 13], contrast of a phase-contrast image is influenced by the MTF of the microscope objective in the same way as that of a 'normal' amplitude object. MTF of a diffraction-limited lens is described by the following formula [20]:

$$T = \frac{2 \left[\arccos(K) - K(1 - K^2)^{1/2} \right]}{\pi}, \quad (3)$$

where T is the MTF value and K is the normalized spatial frequency given by

$$K = v\lambda f^{\#}, \quad (4)$$

where v is the spatial frequency in line pairs per millimetre, λ is the wavelength and $f^{\#}$ is the ratio of the focal length to the diameter of the lens.

With $\lambda = 540$ nm and $S = 1200$ lp mm⁻¹, in the case of the 100 × immersion objective we obtain $K_{100} = 0.222$ and an MTF value $T_{100}^1 = 0.720$. The spatial frequency of the second harmonics is $S_2 = 2400$ lp mm⁻¹, which corresponds to a normalized spatial frequency $K_2 = 0.444$ and $T_{100}^2 = 0.454$. In the case of the third harmonics, $K_3 = 0.666$ and $T_{100}^3 = 0.220$.

So the measured values of ϕ should be divided by these values of T_{100}^i ($i = 1, 2, 3$) respectively to obtain the correct phase differences.

Further correction was made for the MTF of the photographic material. Its value for the film and processing used was $M_f = 0.417$. The formula for the corrected value of the phase difference is

$$\varphi_{\text{corr}} = \frac{\gamma}{2TM_f}. \quad (5)$$

Hence the modulation of the optical path becomes

$$\Delta d = \frac{\varphi_{\text{corr}}\lambda}{2\pi}. \quad (6)$$

Assuming uniform modulation throughout the depth of the holographic emulsion, setting its thickness to $d = 5 \mu\text{m}$ [17], we can determine the refractive index modulation Δn by dividing the Δd values by d .

To determine $\Delta n_1(E_0, V)$, $\Delta n_2(E_0, V)$ and $\Delta n_3(E_0, V)$, that is the first-, second- and third-order refractive index modulations as functions of the bias exposure and fringe visibility, each phase-contrast photomicrograph was Fourier transformed, and then the corresponding spectral amplitudes were determined. The refractive index modulations were obtained using equations (2)–(6).

4. Results and discussion

One of the 84 phase contrast images is shown in figure 1, together with its profile and spectrum. The real size of the photomicrographs was 150 pixels by 3500 pixels. By simply regarding the profile of the grating, one can see a rather regular grating with some fluctuations. The non-sinusoidal shape of the grating is clearly demonstrated by its spectrum. Even the peak belonging to the third harmonic of the grating can be distinguished well (note the logarithmic scale of the ordinate). Bias exposure for this hologram was only $E_0 = 92 \mu\text{J cm}^{-2}$. At higher exposures (a few hundred microjoules per square centimetre), nonlinearity of the recording increases, and a peak corresponding to the fourth harmonic appears in the spectrum. This fact corroborates the results of Slinger *et al.* [9] who, using their higher-order coupled-wave theory, predicted the existence of a small fourth-order harmonic in the profile of the holographic phase gratings studied by them.

The $\Delta n_1(E_0)IV = \text{constant}$ curves belonging to the combination of AAC with R-9 are shown in figure 2. The absolute maximum is 0.027. Δn_1 increases monotonically up to an exposure of about $70 \mu\text{J cm}^{-2}$ at all the visibilities. There are no deep minima, except for some oscillations in the $V = 0.8$ curve. Note that the $V = 1.0, 0.8$ and 0.6 curves almost coincide beyond $E_0 = 600 \mu\text{J cm}^{-2}$. This fact indicates a high degree of nonlinearity.

The highest value of the second-order refractive index modulation is attained around $E_0 = 200 \mu\text{J cm}^{-2}$; it is 0.0044, about 16% of the maximum of Δn_1 (figure 3). Oscillations in the $V = 0.8$ curve can be seen in this figure, too.

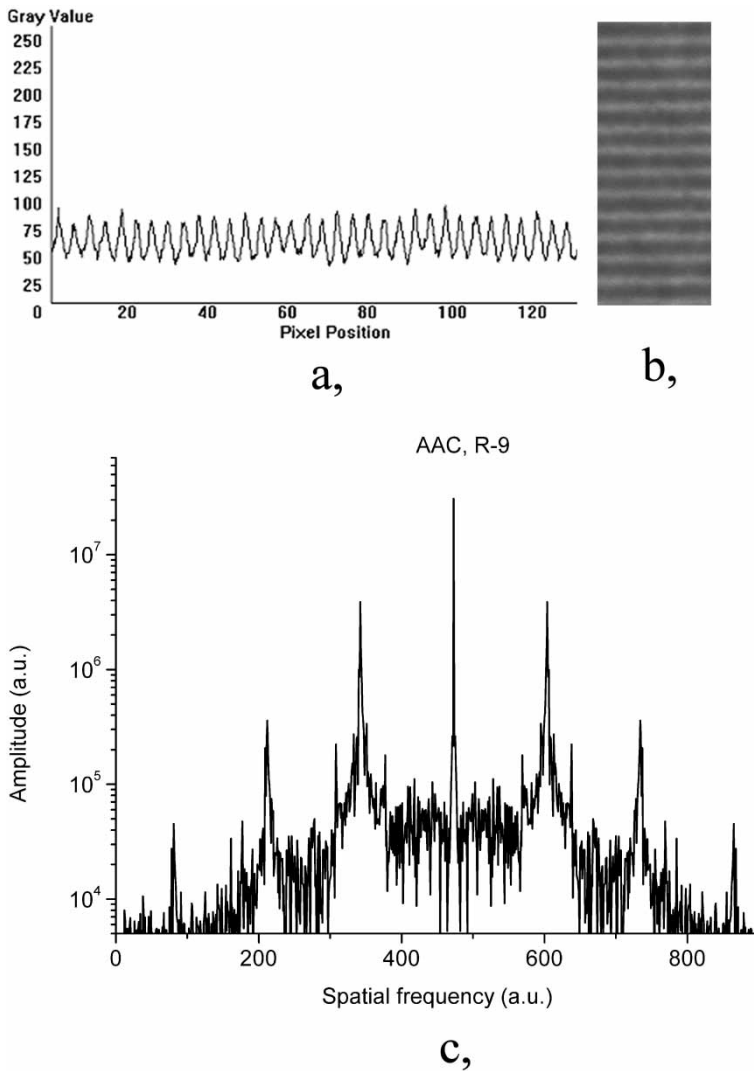


Figure 1. Phase-contrast photomicrograph of (a) a grating, (b) its profile and (c) its spectrum (a.u., arbitrary units) (AAC; R-9; $V = 1.0$; $E_0 = 92 \mu\text{J cm}^{-2}$).

The highest value of the third-order refractive index modulation is attained around $300 \mu\text{J cm}^{-2}$ at $V = 0.8$; it is 0.0012, about 4.4% of the maximum of Δn_1 (figure 4). The curves corresponding to $V = 0.2, 0.6$ and 1.0 are similar; however, at $V = 0.8$ there are strong oscillations. The same experiments performed with other combinations of developers and bleaches gave similar results; so these oscillations cannot be due to any error in the measurements.

To the knowledge of the present author, this work was the first attempt to infer the complete $\Delta n_i(E_0, V)$ ($i = 1, 2, 3$) characteristics of phase gratings from phase-contrast microphotographs.

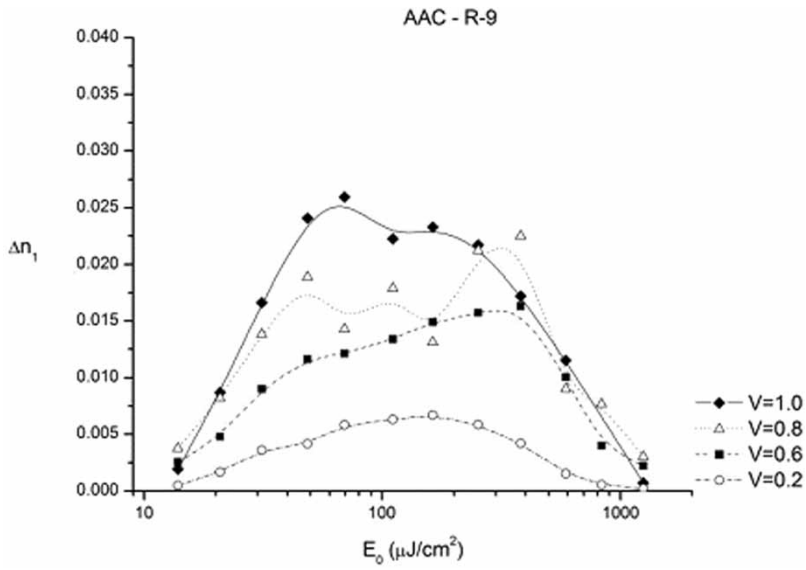


Figure 2. First-order refractive index modulation as a function of bias exposure, at fringe visibility $V=0.2, 0.6, 0.8$ and 1.0 : symbols, data inferred from microphotographs; curves, B -spline fits.

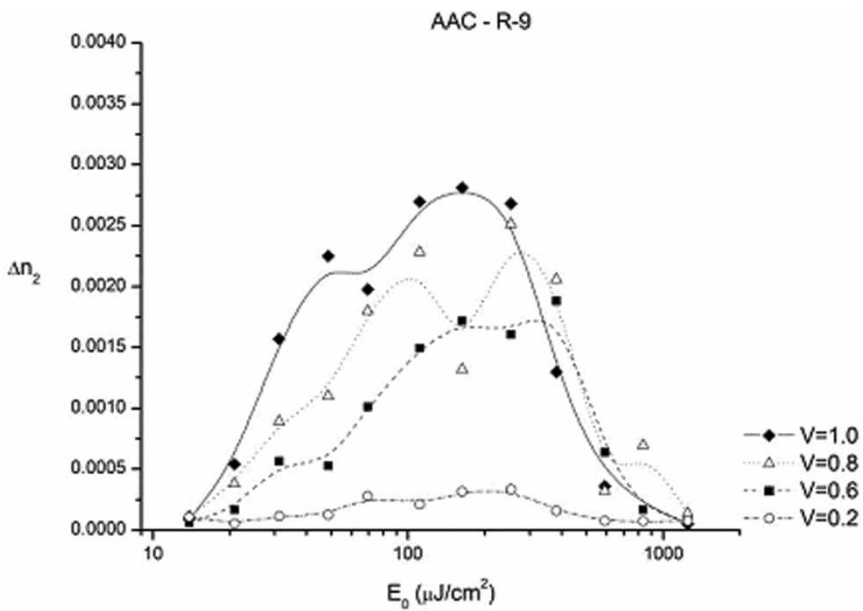


Figure 3. Second-order refractive index modulation as a function of bias exposure, at fringe visibility $V=0.2, 0.6, 0.8$ and 1.0 : symbols, data inferred from microphotographs; curves, B -spline fits.

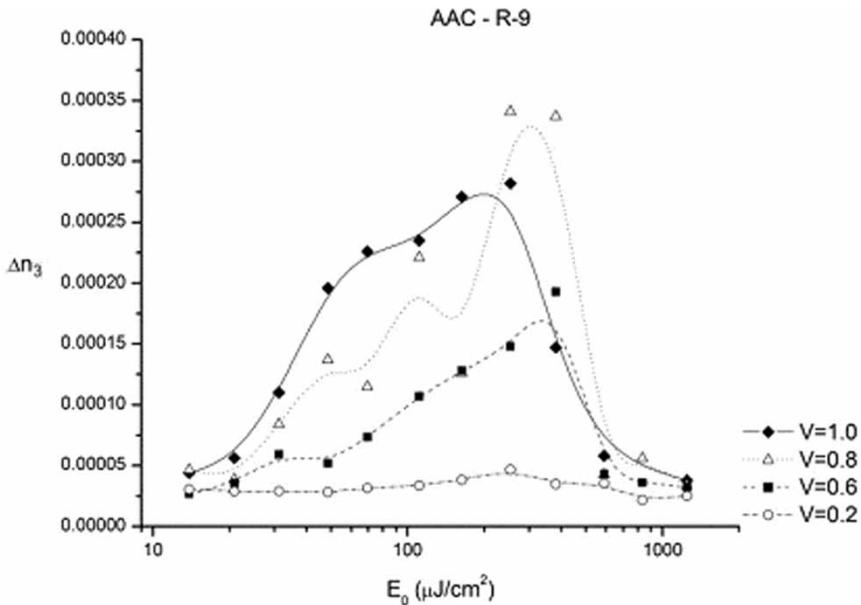


Figure 4. Third-order refractive index modulation as function of bias exposure, at fringe visibility $V=0.2, 0.6, 0.8$ and 1.0 : symbols, data inferred from microphotographs; curves, B -spline fits.

The characteristics obtained in this work can make it possible to calculate the reconstructed image of holographically recorded complex diffractive optical elements using the extension of coupled-wave theory to non-sinusoidal phase gratings, as it was envisaged in the article by Slinger *et al.* [9].

Similar characteristics for other combinations of developers and bleaches used with the same and other recording materials will be available soon; so it will be possible to make comparisons between various processing schemes and recording materials, regarding the fidelity of holographic recording.

Acknowledgment

This research was funded by the Hungarian National Research Fund under grant T 047265.

References

- [1] D. Gabor, *Nature* **161** 777 (1948).
- [2] I. Bányász, G. Kiss and P. Varga, *Appl. Optics* **27** 1293 (1988).
- [3] L.H. Lin, *J. Opt. Soc. Am.* **61** 203 (1971).
- [4] I. Bányász, *Optics Lett.* **18** 658 (1993).

- [5] I. Bányász, *Optics Commun.* **225** 269 (2003).
- [6] H. Kogelnik, *Bell Syst. Tech. J.* **48** 2909 (1969).
- [7] W.W. Rigrod, *J. Opt. Soc. Am.* **64** 97 (1974).
- [8] R. Magnusson and T.K. Gaylord, *J. Opt. Soc. Am.* **67** 1165 (1977).
- [9] C.W. Slinger, R.R.A. Syms and L. Solymar, *Appl. Phys. B* **36** 217 (1985).
- [10] F. Zernike, *Physica* **9** 686, 974 (1942).
- [11] M. Françon, *Microscopie* **1** 115 (1949).
- [12] M. Françon, *Le Contraste de Phase en Optique et en Microscopie* (Editions de la Revue d'Optique Théorique et Instrumentale, Paris, 1950).
- [13] M. Françon, *Progress in Microscopy* (Pergamon, Oxford, 1961).
- [14] R.K. Kostuk and J.W. Goodman, *Appl. Optics* **30** 369 (1991).
- [15] I. Bányász, M. Fried, C. Dücsö and Z. Vértesy, *Appl. Phys. Lett.* **79** 3755 (2001).
- [16] I. Bányász, *Optics Commun.* **192** 27 (2001).
- [17] I. Bányász, *Optics Commun.* **225** 269 (2003).
- [18] I. Bányász, A. Beléndez, I. Pascual and A. Fimia, *J. Mod. Optics* **45** 881 (1998).
- [19] H.I. Bjelkhagen, *Silver-Halide Recording Materials for Holography and Their Processing* (Springer, Berlin, 1993), pp. 93–113.
- [20] M. Laikin, *Lens Design*, Optical Engineering Series, Vol. 48 (Marcel Dekker, New York, 1995).